JOURNAL OF NATURAL PRODUCTS

pubs.acs.org/jnp

Article

Na^+/K^+-ATPase-Targeted Cytotoxicity of (+)-Digoxin and Several Semisynthetic Derivatives

Yulin Ren, Hennrique T. Ribas, Kimberly Heath, Sijin Wu, Jinhong Ren, Pratik Shriwas, Xiaozhuo Chen, Michael E. Johnson, Xiaolin Cheng, Joanna E. Burdette, and A. Douglas Kinghorn*

Cite This: https://dx.doi.org/10.1021/acs.jnatprod.9b01060

Read Online

ACCESS | Metrics & More | Article Recommendations | Supporting Information

ABSTRACT: (+)-Digoxin (**1**) is a well-known cardiac glycoside long used to treat congestive heart failure and found more recently to show anticancer activity. Several known cardenolides (**2**–**5**) and two new analogues, (+)-8(9)-β-anhydrodigoxigenin (**6**) and (+)-17-*epi*-20,22-dihydro-21α-hydroxydigoxin (**7**), were synthesized from **1** and evaluated for their cytotoxicity toward a small panel of human cancer cell lines. A preliminary structure–activity relationship investigation conducted indicated that the C-12 and C-14 hydroxy groups and the C-17 unsaturated lactone unit are important for **1** to mediate its cytotoxicity toward human cancer cells, but the C-3 glycosyl residue seems to be less critical for such an effect. Molecular docking profiles showed that the cytotoxic **1** and the noncytotoxic derivative **7** bind differentially to Na^+/K^+-ATPase. The HO-12β, HO-14β, and HO-3′aα hydroxy groups of (+)-digoxin (**1**) may form hydrogen bonds with the side-chains of Asp121 and Asn122, Thr797, and Arg880 of Na^+/K^+-ATPase, respectively, but the altered lactone unit of **7** results in a rotation of its steroid core, which depotentiates the binding between this compound and Na^+/K^+-ATPase. Thus, **1** was found to inhibit Na^+/K^+-ATPase, but **7** did not. In addition, the cytotoxic **1** did not affect glucose uptake in human cancer cells, indicating that this cardiac glycoside mediates its cytotoxicity by targeting Na^+/K^+-ATPase but not by interacting with glucose transporters.

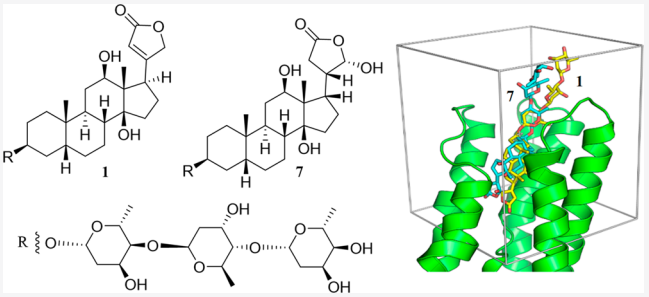

Cardiac glycosides have been investigated extensively for their potential anticancer activities, including cancer cell cytotoxicity, antineoplastic effects in in vivo models, and anticancer activities in clinical trials.[1,2] Among these compounds, (+)-digoxin (**1**), a well-known therapeutic agent isolated originally from the plant *Digitalis lanata* Ehrh. (Plantaginaceae)[3,4] and long used to treat congestive heart failure through inhibition of Na^+/K^+-ATPase,[5] was found to be cytotoxic toward human cancer cell panels, when a large number of compounds were tested in a drug repurposing study.[6]

The potential anticancer activity of (+)-digoxin has been reviewed recently,[1,2,7] with its potent cytotoxicity (IC_{50} 40–200 nM) being reported against a small panel of human cancer cell lines.[8] Interestingly, this cardiac glycoside was also found to synergize the cytotoxicity of cisplatin against human HeLa cervical cancer cells,[9] while cotreatment of paclitaxel with (+)-digoxin resulted in an antagonistic cytotoxicity against HeLa cells.[10] Mechanistically, (+)-digoxin was reported to show anticancer potential through inhibition of Na^+/K^+-ATPase,[11] and it also mediates cancer cell cytotoxicity through induction of autophagy and immunogenic cell death[12,13] and through inhibition of HIF-1α and NF-κB activation.[14,15]

In a driver signaling network identification (DSNI)- and drug functional network (DFN)-based drug repositioning program that integrated multiple types of genomic profiles from patients with groups 3 and 4 medulloblastoma (3 and 4 MB, the most common malignant brain tumor of childhood), (+)-digoxin was characterized as a potential cancer driver signaling inhibitor. Its anti-MB potential has been validated subsequently in both in vitro cell-based assays and in vivo orthotopic patient-derived xenograft models.[16] Unfortunately, the cancer chemotherapeutic features of (+)-digoxin seem not to translate very well in cancer clinical trials,[17] indicating that a more detailed structural investigation might support the design and discovery of new anticancer agents based on (+)-digoxin (**1**).

The importance of the saccharide moiety and the steroid hydroxy groups of several cardiac glycosides in their interaction with the Na^+/K^+-ATPase has been addressed previously.[18] These structural components, along with the C-17 unsaturated heterocycle, were determined as being important in cancer cell cytotoxicity.[19] The cytotoxicity of (+)-digitoxin against a small panel of human cancer cell lines was enhanced by introducing a C_3-MeO*N*-neoglycose unit to the aglycone digitoxigenin,[20]

Special Issue: Special Issue in Honor of Jon Clardy

Received: October 24, 2019

and the C_3-O-neoglycosides of digoxigenin were found to be more cytotoxic than its C_3-MeO*N*-neoglycosides and (+)-digoxin itself when evaluated against NIH H460 human non-small-cell lung cancer cells.[21] Interestingly, when the lactone moiety was replaced with a carboxylic acid group, the cytotoxic activity of the resultant compound was retained,[22] but the inhibitory potencies of (+)-digoxin and 20,22-dihydrodigoxin-21,23-diol were found to be different against RORγt transcriptional activity.[23] A new derivative of (+)-digoxin, namely, BD-4, with a γ-benzylidene group substituted at the C-17-butenolide, exhibited more potent cytotoxicity than the parent compound against HeLa human cervical cancer cells, and this compound mediated its cytotoxicity through a different mechanism of action,[24] as confirmed by the docking profiles, which showed that (+)-digoxin and 21-benzylidene-digoxin targeted Na^+/K^+-ATPase differentially.[25]

In our continuing search for anticancer agents,[26] (+)-digoxin was found to show potent cytotoxicity against a small panel of human cancer cell lines,[27] and (+)-digitoxin, devoid of a 12-hydroxy group, exhibited more potent activity than (+)-digoxin toward human HT-29 colon cancer and MDA-MB-435 melanoma cells.[28] However, (+)-digoxin induced lordosis (spine malformation or curvature disorder) when it was examined in a zebrafish toxicity assay.[29] In the present investigation, two new and several known (+)-digoxin derivatives have been synthesized, of which the mechanism of the generation of the new compounds (+)-8(9)-β-anhydrodigoxigenin (**6**) and (+)-17-*epi*-20,22-dihydro-21α-hydroxydigoxin (**7**) are proposed. The structures of the synthetic compounds have been determined and confirmed by analysis of their spectroscopic data followed by comparison of these data with those of (+)-digoxin, with the ^1H and ^{13}C NMR spectroscopic data of all of these compounds assigned completely. In addition, the cytotoxicity against a small panel of human cancer cell lines of all compounds and the inhibition of Na^+/K^+-ATPase and glucose transport of (+)-digoxin (**1**) have been evaluated, with docking profiles for **1** and its new and noncytotoxic derivative **7** being carried out. The Na^+/K^+-ATPase-related mechanism of action and the relative importance of the hydroxy groups, the C-3 saccharide moiety, and the C-17 unsaturated lactone unit of (+)-digoxin in mediating its cytotoxic activity are also discussed.

RESULTS AND DISCUSSION

It has been reported that both the C-3 saccharide and C-17 unsaturated heterocycle units are of importance for cardiac glycosides to exhibit their cancer cell cytotoxicity,[19] while the sugar moiety and the steroidal hydroxy groups are functional components required for binding between the cardiac glycosides and Na^+/K^+-ATPase.[18] To test the importance of these structural components in effecting the cytotoxicity of (+)-digoxin (**1**), several derivatives (**2**–**7**) were prepared synthetically (Figures S1–S8, Supporting Information) and evaluated biologically.[27,28]

Of these, three acetylated analogues with different numbers of acetyl groups (**2**–**4**) were produced by acetylation of (+)-digoxin (**1**). After **1** was stirred in Ac_2O and pyridine at room temperature for 72 h, (+)-12,4′c-di-*O*-acetyldigoxin (**2**)[30] and (+)-12,3′c,4′c-tri-*O*-acetyldigoxin (**3**)[30] were generated. Both **2** and **3** were separated from a mixture of reaction products, using silica gel column chromatography followed by further purification by passage over Sephadex LH-20. Using the same procedure, (+)-12,3′a,3′b,3′c,4′c-penta-*O*-acetyldigoxin (**4**)[30] was synthesized at 80 °C for 2 h (Scheme 1).

Scheme 1. Synthesis of Compounds 2–4[a]

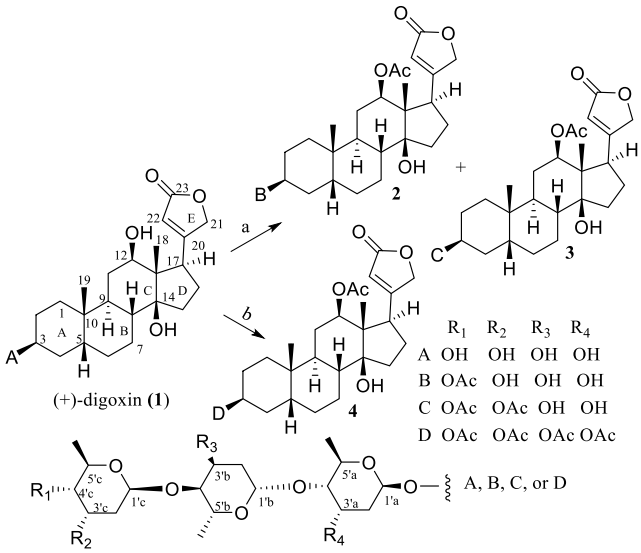

[a]Reagents and conditions: (a) Ac_2O and pyridine, rt, 72 h; (b) Ac_2O and pyridine, 80 °C, 2 h.

Compound **2** showed a sodium adduct ion at *m*/*z* 887.4441 for a molecular formula of $C_{45}H_{68}O_{16}Na^+$, indicating that two hydroxy groups of (+)-digoxin are acetylated. These acetylated groups were proposed at the C-12 and C-4′c positions after comparing the NMR spectroscopic data of **2** with those of (+)-digoxin (Table 1 and Tables S1 and S2, Supporting Information),[31] of which the NMR spectroscopic data have been assigned completely.[32] This assignment for **2** was also confirmed by the HMBC cross-peaks observed between H-12 and H-4′c and their attached acetyl carbonyl groups, respectively (Figure S9, Supporting Information). Similarly, three acetoxy groups were assigned at C-12, C-3′c, and C-4′c of **3**, as indicated by its sodium adduct ion at *m*/*z* 929.4492 ($C_{47}H_{70}O_{17}Na^+$, tri-*O*-acetyldigoxin) and the HMBC correlations between H-12, H-3′c, and H-4′c and their respective acetyl carbonyl groups. Five acetoxy groups were proposed at C-12, C-3′a, C-3′b, C-3′c, and C-4′c of **4**, as supported by its mass spectrometric data (positive-ion HRESIMS *m*/*z* 1013.4761 for $C_{51}H_{74}O_{19}Na^+$) and the HMBC correlations between H-12, H-3′a, H-3′b, H-3′c, and H-4′c and their respective acetyl carbonyl groups (Figure S9, Supporting Information).

When (+)-digoxin (**1**) was reacted with concentrated HCl at room temperature overnight, the compounds (+)-digoxigenin (**5**) and (+)-8(9)-β-anhydrodigoxigenin (**6**) were generated (Scheme 2).[33] These compounds were separated by silica gel column chromatography followed by purification over Sephadex LH-20. Compound **5** was assigned as the aglycone of (+)-digoxin (**1**) by comparing its NMR spectroscopic data with those of **1**, from which the NMR resonances assigned for the saccharide moiety of **1** were found to be absent in **5** (Table 1 and Tables S1 and S2, Supporting Information).[34] This was supported by its positive-ion HRESIMS data at *m*/*z* 413.2336, 390 Da ($C_{18}H_{30}O_9$) less than **1**. A sodium adduct ion at *m*/*z* 395.2211 [18 Da (H_2O) less than **5**] for a molecular formula of $C_{23}H_{32}O_4Na^+$ observed for **6** indicated that this compound

https://dx.doi.org/10.1021/acs.jnatprod.9b01060
J. Nat. Prod. XXXX, XXX, XXX−XXX

Table 1. ^{1}H and ^{13}C NMR Spectroscopic Data of 1 and 7[a]

position	1[b]	1[c]	7[b]	7[c]
1	30.16 CH_2	α 1.29 m	30.25 CH_2	α 1.30 m
		β 1.36 m		β 1.30 m
2	26.00 CH_2	α 1.53 m	25.90 CH_2	α 1.49 m
		β 1.53 m		β 1.49 m
3	72.09 CH	α 3.90 br s	72.20 CH	α 3.88 m
4	29.58 CH_2	α 1.74 m	29.74 CH_2	α 1.67 m
		β 1.33 m		β 1.27 m
5	36.31 CH	β 1.53 m	36.38 CH	β 1.55 m
6	26.43 CH_2	α 1.18 m	26.20 CH_2	α 1.08 m
		β 1.72 m		β 1.73 m
7	21.35 CH_2	α 1.08 m	21.08 CH_2	α 1.02 m
		β 1.69 m		β 1.61 m
8	40.47 CH	β 1.44 m	36.81 CH	β 1.44 m
9	31.61 CH	α 1.59 m	31.58 CH	α 1.64 m
10	34.67 C		34.82 C	
11	29.70 CH_2	α 1.41 m	28.69 CH_2	α 1.38 m
		β 1.06 m		β 1.21 m
12	72.96 CH	α 3.23 m	68.15 CH	α 3.36 m
13	55.70 C		49.93 C	
14	84.33 C		85.66 C	
15	32.42 CH_2	α 1.88 m	28.46 CH_2	α 1.87 m
		β 1.61 m		β 1.50 m
16	26.79 CH_2	α 1.98 m β 1.84 m	19.87 CH_2	α 1.67 m β 1.53 m
17	45.18 CH	α 3.26 m	42.88 CH	β 2.06 m
18	9.44 CH_3	β 0.65 s	9.84 CH_3	β 0.89 s
19	23.67 CH_3	β 0.85 s	23.63 CH_3	β 0.87 s
20	176.94 C		39.28 CH	β 2.10 m
21	73.31 CH_2	β 4.85 overlapped (17.9)	94.16 CH	β 4.40 m
		α 4.94 br d (17.9)		
22	115.83 CH	5.82 br s	35.06 CH_2	α 2.30 m
				β 2.03 m
23	173.96 C		174.17 C[d]	
1′a	95.32 CH	α 4.78 m	95.39 CH	α 4.77 m
2′a	38.45 CH_2	α 1.77 m	38.47 CH_2	α 1.76 m
2′a		β 1.56 m		β 1.53 m
3′a	66.27 CH	β 4.03 m	66.31 CH	β 4.04 m
4′a	81.67 CH	β 3.14 m	81.69 CH	β 3.13 m
5′a	67.49 CH	α 3.70 m	67.52 CH	α 3.69 m
6′a	18.03 CH_3	β 1.10 d (7.0)	18.06 CH_3	β 1.09 d (5.8)
1′b	99.09 CH	β 4.80 m	99.12 CH	β 4.79 m
2′b	37.92 CH_2	α 1.64 m	37.95 CH_2	α 1.60 m
		β 1.84 m		β 1.83 m
3′b	66.13 CH	α 4.05 m	66.16 CH	α 4.05 m
4′b	81.92 CH	α 3.11 m	81.94 CH	α 3.11 m
5′b	67.61 CH	β 3.76 m	67.64 CH	β 3.73 m
6′b	18.03 CH_3	α 1.12 d (7.0)	18.06 CH_3	α 1.11 d (6.1)
1′c	99.00 CH	α 4.83 m	99.02 CH	α 4.81 m
2′c	38.31 CH_2	α 1.87 m	38.34 CH_2	α 1.86 m
		β 1.59 m		β 1.58 m
3′c	67.01 CH	β 3.85 m	67.03 CH	β 3.84 m
4′c	72.67 CH	β 3.02 m	72.70 CH	β 2.99 m
5′c	69.05 CH	α 3.66 m	69.08 CH	α 3.64 m
6′c	18.37 CH_3	β 1.13 d (5.7)	18.40 CH_3	β 1.12 d (5.6)
OH-12		β 4.63 s		β 4.34 br s
OH-14		β 4.12 s		β 4.07 br s
OH-21				α 3.67 m
OH-3′a		α 4.22 s		α 4.21 br s
OH-3′b		β 4.28 s		β 4.28 br s
OH-3′c		α 4.65 s		α 4.63 br s
OH-4′c		α 4.61 s		α 4.61 br s

[a]Assignments of chemical shifts are based on the analysis of 1D and 2D NMR spectra. The ^{13}C NMR spectroscopic data CH_3, CH_2, CH, and C multiplicities were determined by DEPT 90, DEPT 135, and HSQC experiments, and the overlapped ^{1}H NMR signals were assigned from $^{1}H-^{1}H$ COSY, HSQC, and HMBC spectra without designating multiplicity. [b]The ^{13}C NMR spectroscopic data (δ) were measured in DMSO-d_6 at 100.61 MHz and referenced to the solvent residual peak at δ 39.52.[31] [c]The ^{1}H NMR spectroscopic data (δ) were measured in DMSO-d_6 at 400.13 MHz and referenced to the solvent residual peak at δ 2.50.[31] [d]Shown in the 2D HMBC NMR spectra.

Scheme 2. Synthesis of Compounds 5 and 6[a]

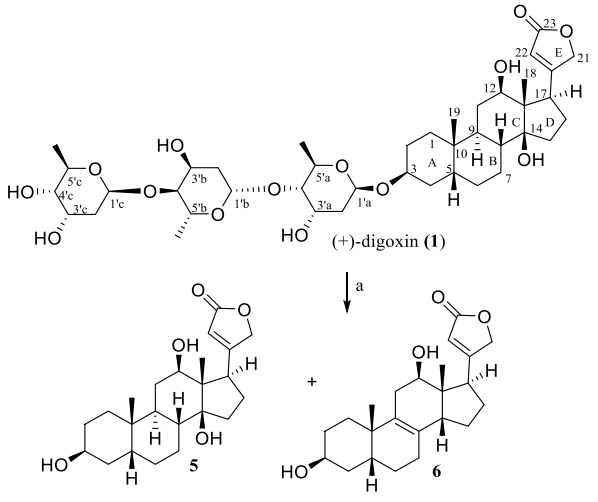

[a]Reagents and conditions: (a) concentrated HCl, rt, overnight.

is a dehydrated analogue of **5**, as inferred from its NMR resonances at δ_C 128.13 for C-8 and at δ_C 131.57 for C-9 but not at δ_C 40.51 and δ_C 31.50 for the respective carbons of **5**. This assignment has been supported by the HMBC correlations observed between H_3-18 and C-12, C-13, C-14, and C-17 and between H_3-19 and C-1, C-5, C-9, and C-10, as well between H-11 and C-8 and between H-16 and C-14 of **6** (Figures S8–S10 and Tables S1 and S2, Supporting Information). A plausible mechanism for the generation of **6** from **1** could involve an acid-mediated hydrolysis of **1** to form **5** and a 1,2-hydride shift concurrent with hydration of **5** (Scheme 3).

Another new analogue, (+)-17-*epi*-20,22-dihydro-21α-hydroxydigoxin (**7**), was produced when (+)-digoxin (**1**) was stirred in NaOH-saturated MeOH at 60 °C overnight (Scheme 4). Comparison of the NMR spectroscopic data of **7** with those of **1** indicated these compounds to contain the same saccharide moiety and A/B/C/D-ring system, but a different lactone unit. Compound **7** gave a sodium adduct ion at *m/z* 821.4299 for a molecular formula of $C_{41}H_{66}O_{15}Na^+$, 18 Da (H_2O) more than **1**, indicating that this derivative is a hydration product of **1**. In turn, the $\Delta^{20(22)}$ double bond in **1** was saturated in **7**, with a hydroxy group being substituted at C-21, as supported by its ^{13}C NMR spectroscopic resonances at δ_C 39.28 (C-20), 94.16 (C-21), and 35.06 (C-22), as compared to those at δ_C 176.94 (C-20), 73.31 (C-21), and

https://dx.doi.org/10.1021/acs.jnatprod.9b01060
J. Nat. Prod. XXXX, XXX, XXX−XXX

Scheme 3. Plausible Mechanism for the Generation of (+)-8(9)-β-Anhydrodigoxigenin (6) from (+)-Digoxin (1)

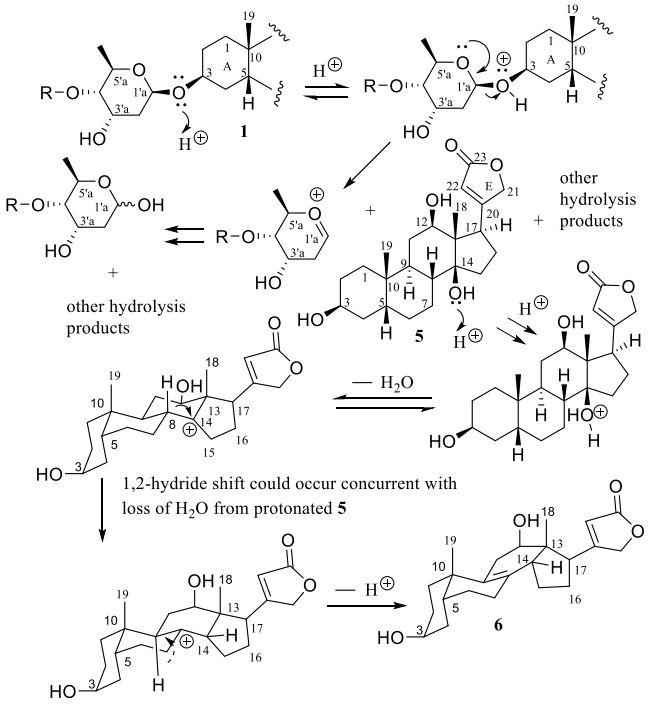

Scheme 4. Synthesis of Compound 7[a]

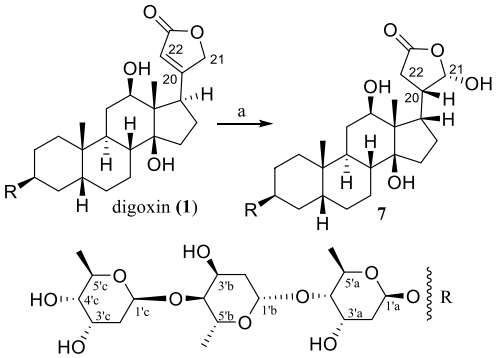

[a]Reagents and conditions: (a) MeOH saturated with NaOH, 60 °C, overnight.

115.83 (C-22) in **1** (Table 1). The stereostructure of **7** was assigned by analysis of its specific rotation value and 1D and 2D NMR spectra, which indicated that **7** and **1** have the same configuration for their glycosidic moiety and A-, B-, and C-ring system but differ in the D-ring and lactone unit. This was supported by the 2D NOESY correlations between H-17 and H-7β, H-16β, and H_3-18, between H-20 and H-7β, H-16β, and H_3-18, and between H-21 and H-7β, H-16β, and H-20 in **7** (Figure S10, Supporting Information). Thus, **7** was determined as having a β-oriented proton at C-17, C-20, and C-21, as implied by its ^{13}C NMR spectroscopic resonances at δ_C 28.69, 68.15, 49.93, 85.66, 28.46, 19.87, 42.88, and 9.84, rather than at δ_C 29.70, 72.96, 55.70, 84.33, 32.42, 26.79, 45.18, and 9.44 in **1** for their respective C-11−C-18 carbons (Table 1), due to the effects from the different orientation of the C-17 lactone unit.[35,36]

A plausible mechanism for the generation of **7** from **1** could involve a base-mediated isomerization of C-17 to form isomer **1i** and deconjugation of the unsaturated lactone **1i** followed by opening of the resulting β,γ-unsaturated lactone unit and a subsequent hydration of the resulting formyl group followed by cyclization of the intermediate hydrate (or derivatives) (Scheme 5).

Scheme 5. Plausible Mechanism for the Formation of (+)-17-*epi*-20,22-Dihydro-21α-hydroxydigoxin (7) from (+)-Digoxin (1)

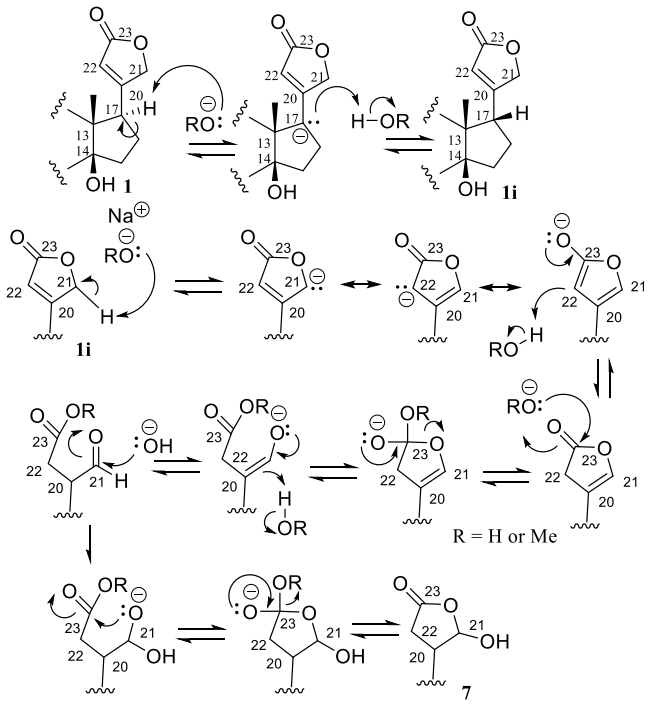

The structure of (+)-digoxin (**1**) was established previously by analysis of its single-crystal X-ray diffraction data,[4] with the (3′c*S*,4′c*S*) absolute configuration determined from its $[Mo_2(OAc)_4]$-induced ECD.[27] In turn, its (3*S*, 5*R*, 8*R*, 9*S*, 10*S*, 12*R*, 13*S*, 14*S*, 17*R*, 1′a*R*, 3′a*S*, 4′a*S*, 5′a*R*, 1′b*S*, 3′b*S*, 4′b*S*, 5′b*R*, 1′c*S*, 3′c*S*, 4′c*S*, 5′c*R*) absolute configuration was determined and supported by the 2D NOESY NMR spectrum (Figure S10, Supporting Information). Following this determination, the (3*S*, 5*R*, 8*R*, 9*S*, 10*S*, 12*R*, 13*S*, 14*S*, 17*R*) absolute configuration for the steroid core was assigned for compounds **2**−**5**, with those for their glycosyl unit being defined as (1′a*R*, 3′a*S*, 4′a*S*, 5′a*R*, 1′b*S*, 3′b*S*, 4′b*S*, 5′b*R*, 1′c*S*, 3′c*S*, 4′c*S*, 5′c*R*) for **2**, (1′a*R*, 3′a*S*, 4′a*S*, 5′a*R*, 1′b*S*, 3′b*S*, 4′b*S*, 5′b*R*, 1′c*S*, 3′c*S*, 4′c*R*, 5′c*R*) for **3**, and (1′a*R*, 3′a*S*, 4′a*R*, 5′a*R*, 1′b*S*, 3′b*S*, 4′b*R*, 5′b*R*, 1′c*S*, 3′c*S*, 4′c*R*, 5′c*R*) for **4**. In addition, the (3*S*, 5*R*, 10*S*, 12*R*, 13*S*, 14*R*, 17*R*) and (3*S*, 5*R*, 8*R*, 9*S*, 10*S*, 12*R*, 13*S*, 14*S*, 17*S*, 20*S*, 21*S*, 1′a*R*, 3′a*S*, 4′a*S*, 5′a*R*, 1′b*S*, 3′b*S*, 4′b*S*, 5′b*R*, 1′c*S*, 3′c*S*, 4′c*S*, 5′c*R*) absolute configurations were assigned for compounds **6** and **7**, from analysis of their specific rotation values and ECD (Figure 1) and 2D NOESY NMR spectroscopic data and from comparison of all of these data with those of (+)-digoxin (**1**) (Figures S8−S10, Supporting Information).

As shown in Figure 1, the positive Cotton effect (CE) around 241 nm shown in the ECD spectrum of (+)-digoxin (**1**) was absent in the ECD spectrum of **7**, due to the loss of the α,β-unsaturated lactone functional unit in **7**. The ECD spectrum of **5** was found to be closely comparable with that of

https://dx.doi.org/10.1021/acs.jnatprod.9b01060
J. Nat. Prod. XXXX, XXX, XXX−XXX

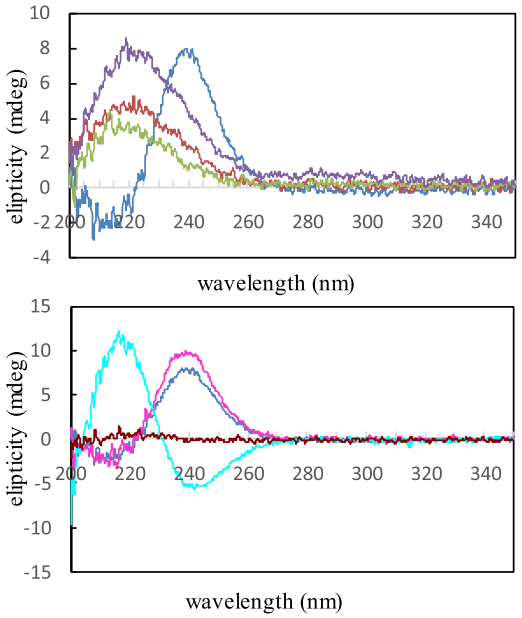

Figure 1. ECD spectra of compounds **1** (blue), **2** (red), **3** (green), and **4** (purple) (upper) and those of compounds **1** (blue), **5** (pink), **6** (aqua), and **7** (burgundy) (below). The data were obtained in HPLC-grade MeOH as the average of three scans corrected by subtracting a spectrum of the appropriate solution in the absence of the samples recorded under identical conditions. Each scan in the range 200−450 nm was obtained by taking points every 0.1 nm with a 50 nm/min scanning speed and a 1 nm bandwidth. No Cotton effects were observed in the range 350−450 nm.

(+)-digoxin (**1**), indicating that the glycosyl unit present does not affect the ECD curve of **1** (Figure 1). A (17*R*) configuration was assigned for compounds **2**−**4** from their 2D NOESY NMR spectra and specific rotation values, which are consistent with those of **1**. However, around a 20 nm shift was found in the positive CEs (in the range 213−221 nm) for **2**−**4** when compared with that around 241 nm for (+)-digoxin (**1**), indicating that an acetoxy group at C-12 results in the ECD spectrum of (+)-digoxin being modified. In addition, a (17*R*) configuration was indicated for **6** from its consistent 2D NOESY correlations with those of **5** and from its sequential negative and positive CEs at 241.8 and 216.1 nm in the ECD spectrum. These reversed CEs of **6** may result from the B-/C-/D-ring conformational change upon formation of the C-8/C-9 double bond.[27] Thus, the presence of a double bond in the B-/C-/D-ring system could reverse the CEs observed for this type of cardiac glycosides.

Based on the established NMR spectroscopic assignments of (+)-digoxin (**1**),[32] the ^{1}H and ^{13}C NMR spectroscopic data of the synthetic cardiac glycosides **2**−**7** presented herein were assigned completely, by analysis of their 1D and 2D NMR spectra (Table 1 and Tables S1 and S2, Supporting Information).

Compounds **1**−**7** were evaluated for their cytotoxicity against human HT-29 colon, MDA-MB-231 breast, and OVCAR3 ovarian cancer and MDA-MB-435 melanoma cells, using a protocol reported previously, with paclitaxel as the positive control.[28] This appears to be the first report of the cytotoxicity of compounds **2**−**7** toward these cancer cell lines. The parent compound, (+)-digoxin (**1**), exhibited potent cytotoxicity toward all the cell lines tested, with IC_{50} values in the range 0.1−0.3 μM (Table 2). The aglycone **5** was also

Table 2. Cytotoxicity of 1−7[a]

compound	HT-29[b]	MDA-MB-231[c]	OVCAR3[d]	MDA-MB-435[e]
1	0.28	0.31	0.10	0.17
2	5.1	8.2	2.5	5.4
3	>10	>10	6.2	>10
4	>10	>10	8.2	>10
5	3.6	3.2	2.4	0.9
6	>10	>10	>10	>10
7	>10	>10	>10	>10
(+)-digitoxin[f]	0.068	0.48	0.12	0.043
paclitaxel[g]	0.0008	0.0027	0.0033	0.0002

[a]IC_{50} values are the concentration (μM) required for 50% inhibition of cell viability for a given test compound with a 72 h treatment and were calculated using nonlinear regression analysis with measurements performed in triplicate and representative of three independent experiments, where the values generally agreed within 10%. [b]IC_{50} value toward the HT-29 human colon cancer cell line. [c]IC_{50} value toward the MDA-MB-231 human breast cancer cell line. [d]IC_{50} value toward the OVCAR3 human ovarian cancer cell line. [e]IC_{50} value toward the MDA-MB-435 human melanoma cell line. [f]Data reported previously.[28] [g]Positive control.

found to exhibit activity toward these cells, with IC_{50} values in the range 0.9−3.6 μM (Table 2), indicating that the glycosyl unit is not critical for **1** to mediate cellular cytotoxicity. However, the cytotoxicity against all of these cell lines decreased in the sequence **2**, **3**, and **4**, and no discernible activity was observed for compounds **6** and **7** (Table S3, Supporting Information). This indicates that *O*-acetylation reduces the cytotoxicity of (+)-digoxin (**1**), and either removal of its C-14 hydroxy group followed by unsaturation of the C-8 and C-9 bond or inversion of its C-17 configuration followed by saturation of the lactone unit and introducing simultaneously a hydroxy group at C-21 results in activity being abolished. Thus, the C-12 and C-14 hydroxy groups and C-17 lactone unit seem to be important for **1** to mediate its cytotoxicity against human cancer cells and to interact with its molecular targets.

It is well known that Na^+/K^+-ATPase is a potential target for cardiac glycosides to mediate their antitumor properties,[11] and the U-shaped *cis*−*trans*−*cis* fused steroid core (steroid core), the β-oriented C-14 hydroxy group (HO-14β), the C-17 five-membered unsaturated lactone unit (17β-lactone), and the C-3 carbohydrate moiety (3β-glycosyl) are all critically important for these compounds to bind to Na^+/K^+-ATPase.[18,24,25] The crystal structure of Na^+/K^+-ATPase and bound ouabain [a hydroxylated analogue of (+)-digoxin] at a low affinity showed that this cardenolide binds to a cavity formed by the transmembrane helices M1, M2, M4, M5, and M6 that are close to the K^+-binding sites of Na^+/K^+-ATPase.[37] Ouabain inserts deeply into the transmembrane domain, with the steroid core being held tightly in a cavity lined by the M4−M6 helices. Hydrogen bonds were found to be formed between the HO-14β and 3β-glycosyl and Thr-804 and Arg-887 (in the L7/8 loop and Glu-319 on M4), respectively, and the 17β-lactone docked closely to Val-329 and Ala-330 in the M4E helix, indicating that the position of the conjugated carbonyl group in the 17β-lactone is important.[37]

In the crystal structure for a complex of Na^+/K^+-ATPase and ouabain at a high affinity state, an extensive hydrogen-bonding network formed between HO-5β, HO-14β, and HO-19β of ouabain and Glu117 (αM2), Thr797 (αM6), and Gln111 (αM1) and Asn122 (αM2) of Na^+/K^+-ATPase, respectively,

https://dx.doi.org/10.1021/acs.jnatprod.9b01060
J. Nat. Prod. XXXX, XXX, XXX−XXX

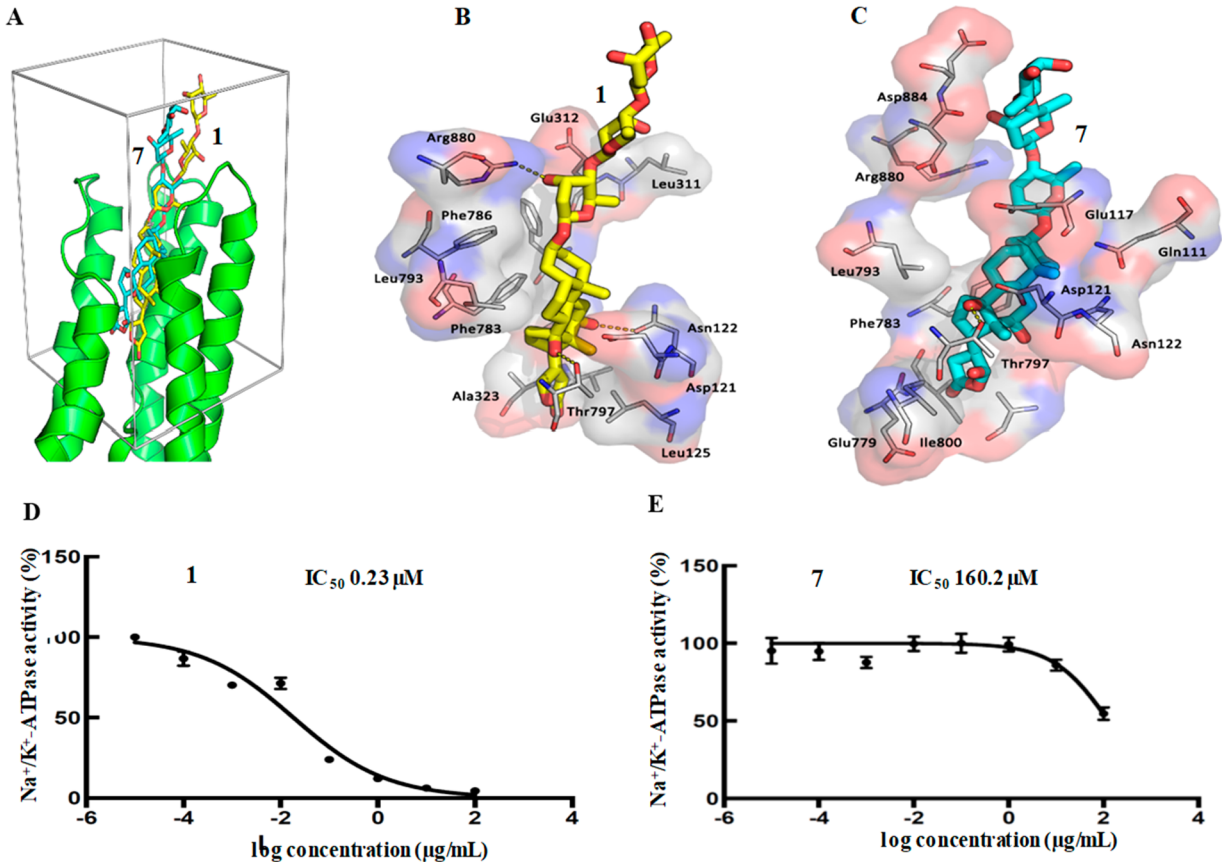

Figure 2. Docking box and the predicted binding pose of **7** (cyan sticks) from docking aligned with (+)-digoxin (**1**) (yellow sticks, from the crystal structure) (A), and binding poses of **1** (yellow sticks, from the crystal structure) (B) and **7** (cyan sticks, predicted) (C) in the Na^+/K^+-ATPase pocket, and inhibition of Na^+/K^+-ATPase by **1** (D) and **7** (E).

was reported.[38] The 3β-attached glycosyl moiety of ouabain was found to occupy a wide cavity lined with polar residues, including Glu116 (loop αM1−2), Glu312 (αM4), Arg880, and Asp884 (loop αM7−8), with the 17β-affixed lactone unit being located in a hydrophobic funnel composed of Leu125 (αM2), Ala323 (αM4), and Ile800 (αM6).[38] Following this, the crystal structure of the E2P form of the pig kidney Na^+/K^+-ATPase ($\alpha1\beta1\gamma$) in complex with (+)-digoxin (**1**) was adopted, which showed that the HO-14β of **1** and the Thr797 (αM6) side-chain of Na^+/K^+-ATPase could be within hydrogen bond distance, and HO-12β forms a hydrogen bond with Asn122 (αM2). The first proximal digitoxose unit of (+)-digoxin (**1**) is located in a wide cavity lined with polar residues Gln111, Thr114, Glu116, Gln117 (loop αM1−2), Glu312 (αM4), Arg880 (loop αM7−8), and Gln84 (β-ectodomain), and similarly to ouabain, its 17β-lactone unit occupies a hydrophobic funnel formed by Leu125 (αM2), Ala323 (αM4), and Ile800 (αM6).[39] This indicated that the HO-12β, HO-14β, 3β-glycosyl, and the 17β-attached lactone unit are all important for (+)-digoxin (**1**) to bind to Na+/K+-ATPase, consistent with the previous conclusions from the crystal structures of the complex of Na^+/K^+-ATPase and ouabain.[37,38]

In the present work, computer-simulated docking profiles for the cytotoxic (+)-digoxin (**1**) and its noncytotoxic analogue, (+)-17-*epi*-20,22-dihydro-21α-hydroxydigoxin (**7**), were investigated. In contrast to **1**, for which the 17β-lactone and steroid core overlaid the crystal structure very well, **7** seemed not to fit into the cation-binding site of Na^+/K^+-APTase. Only 28 out of 320 (8.75%) final predicted binding poses of **7** oriented in a way that the lactone unit penetrates deep inside the hydrophobic funnel formed by α-M4−M6, where the 17β-lactone unit of **1** binds to the protein (Figure 2A). The relative orientation between the lactone and the steroid moieties of **7** is opposite to that of **1**, and thus, if **7** adopts a similar pose to **1**, it would clash with the αM4 helix (Figure 2B and C). In addition, the lactone unit of **7** rotates away from the cation-binding site of Na^+/K^+-ATPase to assume a different pose, with the carbonyl group being directed to a small groove on the side of the pocket made by Ile320, Ala323 (αM4) and Ile780, Phe783 (αM5) (Figure 2C). This rotation makes enough room for its HO-21α substituent to occupy this site, but the presence of this group impairs the binding of **7** to the hydrophobic groove.

The nonpolar concave α-surface of the steroid core of **7** interacts with bulky hydrophobic side chains of αM4−M6 (Figure 2C), which constitute a generally conserved docking platform for most cardiac glycosides, including (+)-digoxin (4RET), bufalin (4RES),[39] and ouabain (4HYT).[38] The hydroxy groups on the β-surface of (+)-digoxin (**1**) could form hydrogen bonds with the side-chains of Asp121 (αM2) and Asn122 (αM2) (HO-12β) and Thr797 (αM6) (HO-14β) of Na^+/K^+-ATPase (Figure 2B). However, upon rotation of the lactone unit of **7**, its steroid core is also rotated by nearly 30° and is oriented toward the entrance of the hydrophobic cavity. This results in the hydrogen bonds between HO-12β of **7** and Na^+/K^+-ATPase being lost (Figure 2C), which, in turn, weakens the binding between **7** and the protein, and thus, it

https://dx.doi.org/10.1021/acs.jnatprod.9b01060
J. Nat. Prod. XXXX, XXX, XXX−XXX

does not show any positive activities in the cytotoxicity assays (Table 2).

Similarly, (+)-digoxin (**1**) has a sterically unfavorable HO-12β substituent, which could have an impact on its binding to Na^+/K^+-ATPase,[37] and thus, it showed a decreased binding affinity and cancer cell cytotoxicity when compared with (+)-digitoxin.[27,28,40] Introducing a 3β-glycosyl unit to the steroid core of a cardenolide could fill the large vacant space around the glycosyl residue to enhance the binding affinity, and thus **1** was found to show a more potent inhibitory activity against Na^+/K^+-ATPase than its aglycone[40] and exhibited more potent cytotoxicity toward human cancer cells than (+)-digoxigenin (**5**) (Table 2).

To test the effect of the C-17 configuration on the binding between **7** and Na^+/K^+-ATPase, a docking profile was produced for its 17,20,21-triepimer (**7a**), which showed that the binding between **7** or **7a** and Na^+/K^+-ATPase is different (Figure 2 and Figure S11, Supporting Information). Unlike **7**, compound **7a** binds to Na^+/K^+-ATPase in a similar way to (+)-digoxin (**1**). However, the HO-21β of **7a** was found to be surrounded by several hydrophobic residues within a 5 Å distance, including L125 and I800 of Na^+/K^+-ATPase (Figure S11, Supporting Information), which could negatively impact the binding between **7a** and Na^+/K^+-ATPase.[41] Also, a negative effect may occur for HO-21β to dock a hydrophobic pocket, due to the effect of desolvation.[41] Thus, **7a** could bind to Na^+/K^+-ATPase, but the binding is not as strong as **1**, indicating that the substituent, configuration, and conformation of the C-17 lactone unit all affect the binding between cardiac glycosides and Na^+/K^+-ATPase.

It has been reported previously that (+)-digoxin (**1**) inhibits potently Na^+/K^+-ATPase activity,[42] and the substituents at C-10, C-12, and C-17 of the steroid core of **1** or other cardiac glycosides could affect critically this enzyme inhibitory effect.[43] Thus, the cytotoxic (+)-digoxin (**1**) and its noncytotoxic analogue, (+)-17-*epi*-20,22-dihydro-21α-hydroxydigoxin (**7**), were tested for their ability to inhibit Na^+/K^+-ATPase activity herein. The cellular enzyme adenosine 5′-triphosphatase from the porcine cerebral cortex was treated with various concentrations of both cardiac glycosides, and, as expected, **1** inhibited Na^+/K^+-ATPase activity in a concentration-dependent manner, with an IC_{50} value of 0.23 μM (Figure 2C), but **7** did not at concentrations less than 100 μM (IC_{50} 160.2 μM) (Figure 2D), indicating that the cytotoxicity of **1** could result from its Na^+/K^+-ATPase inhibitory activity.

Na^+/K^+-ATPase is an electrogenic pump located in the cell membrane to transport potassium ions in and sodium ions out. Inhibition of this pump could result in a higher intracellular Na^+/K^+ ratio followed by a prevented calcium ion exit and a resultant higher concentration of cytoplasmic Ca^{2+}. This, in turn, increases calcium uptake into the sarcoplasmic reticulum by the sarco/endoplasmic reticulum (ER) calcium ATPase2 (SERCA2) transporter and leads to tumor cell apoptosis through cell cycle arrest and caspase activation.[44] In addition, Na^+ was found to be required in the extracellular solutions to drive uphill glucose transport, for which the energy is provided by the sodium gradient maintained by the Na^+/K^+-ATPase across the brush-border membrane, and Na^+/glucose cotransporters (SGLTs) depend critically on the stoichiometry of the Na^+ and sugar fluxes to accumulate sugar.[45] Both the Na^+/K^+-ATPase membrane protein and SERCA pump were found to play an important role in the uptake of glucose,[46,47] indicating that the sugar pump could be closely related to the Na^+ pump. This was supported by ouabain and thevetin, two cardiac glycosides showing inhibitory effects on the active transport of 3-methylglucose across the intestine of frogs in vitro.[48]

Cancer cells require an increase in glucose uptake and metabolism to meet the energy and biomass synthesis for their fast proliferation rates,[49] and these cells take in the majority of glucose via glucose transporters, which have become important targets for the development of anticancer agents.[50,51] Using a procedure reported previously,[52] (+)-digoxin (**1**) was tested for its effects on glucose uptake in H1299 human lung cancer cells, against which **1** showed potent cytotoxicity, with an IC_{50} value of 0.46 μM (Figure 3). However, the results showed that

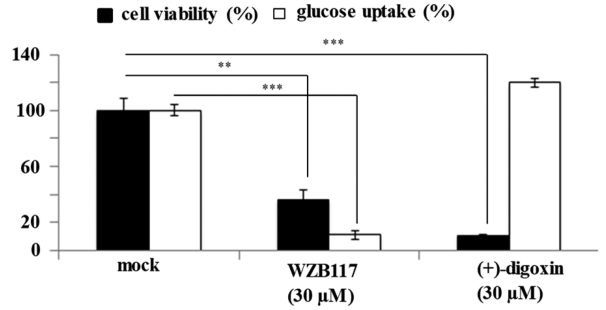

Figure 3. Cytotoxicity against H1299 cells and glucose transport inhibition of **1**. H1299 human lung cancer cells were treated by vehicle, WZB117 (30 μM, positive control), or (+)-digoxin (30 μM) for 15 min. After glucose uptake was initiated by 2-deoxy-D-[^{3}H]glucose, cells were lysed and the radioactivity of the cell lysates was measured. The results showed that (+)-digoxin showed cytotoxicity toward H1299 cells (IC_{50} 0.46 μM), but it did not inhibit glucose transport (columns, means, $n = 3$; bars, SE; $^{**}p \leq 0.01$ and $^{***}p \leq 0.001$ when compared with the values from mock).

1 did not inhibit glucose uptake in H1299 cells (Figure 3), indicating that this cardiac glycoside mediates its cytotoxicity toward H1299 cells through a molecular signaling process exclusive of glucose transport. Similar evidence has been obtained previously, which showed that excretion of Ca^{2+}, Mg^{2+}, and PO_4^{3-} by the ipsilateral kidney was enhanced by (+)-digoxin (**1**), but no change in the maximal transport of glucose was observed at the dose levels studied when 12−27 kg female dogs were renal-artery infused by (+)-digoxin (**1**) (0.05−0.08 mg/kg). This suggested that cardiac glycosides may affect renal tubular excretion of inorganic phosphate differently when compared with that of glucose.[53]

Therefore, (+)-digoxin (**1**) targets Na^+/K^+-ATPase to mediate its cytotoxicity, as evidenced by the inhibition of Na^+/K^+-ATPase observed for **1** but not for its noncytotoxic derivative **7** and by the presence of the important HO-14β and 17β-lactone functionalities in mediating its cytotoxicity and in its binding to Na^+/K^+-ATPase.

There are serious challenges for the development of (+)-digoxin (**1**) as a new anticancer drug, including its narrow clinic therapeutic index[54] and poor clinical outcomes,[17] of which both could result from the inhibition of Na^+/K^+-ATPase of **1**.[1] In the present study, both HO-14β and the 17β-lactone moiety were characterized as important structural components for mediation of the cytotoxicity of **1** and in the binding between this cardiac glycoside and Na^+/K^+-ATPase. In addition, the Na^+/K^+-ATPase inhibitory activity of **1** was found to be blocked by synthetic derivatization of its 17β-lactone unit to produce **7**. These indicate that modifications of

https://dx.doi.org/10.1021/acs.jnatprod.9b01060
J. Nat. Prod. XXXX, XXX, XXX−XXX

either the HO-14β or the 17β-lactone moiety of (+)-digoxin (**1**) could generate new compounds that target Na^+/K^+-ATPase differentially or orient different targets to improve the therapeutic index and clinical trial outcomes of **1**.

EXPERIMENTAL SECTION

General Experimental Procedures. Optical rotations were measured at room temperature on an Anton Paar polarimeter (Anton Paar, Graz, Austria). UV spectra were recorded on a Hitachi U2910 ultraviolet spectrophotometer. ECD measurements were performed using a JASCO J-810 spectropolarimeter. IR spectra were recorded on a Nicolet 6700 FT-IR spectrometer. ^{1}H and ^{13}C, DEPT 90, DEPT 135, HSQC, HMBC, NOESY, and COSY NMR spectra were recorded at room temperature on a Bruker Avance II 400, Bruker Avance III HD 700, or Bruker Avance III HD 800 MHz NMR spectrometer. ESIMS or HRESIMS data were collected on a Bruker Maxis 4G Q-TOF mass spectrometer in the positive-ion mode. Column chromatography was conducted using silica gel (65 × 250 or 230 × 400 mesh, Sorbent Technologies, Atlanta, GA, USA). Analytical TLC was performed on precoated silica gel 60 F254 plates (Sorbent Technologies). Sephadex LH-20 was purchased from Amersham Biosciences, Uppsala, Sweden. For visualization of TLC plates, H_2SO_4 was used as a spray reagent. All procedures were carried out using solvents purchased from commercial sources and employed without further purification. (+)-Digoxin, paclitaxel, and other reagents for chemical synthesis were purchased from Sigma-Aldrich (St. Louis, MO, USA) (purity ≥98%).

Acetylation of (+)-Digoxin (1). To a 25 mL glass vial equipped with a magnetic stirrer, containing 14.1 mg (0.018 mmol) of (+)-digoxin (**1**), were added 50 μL of Ac_2O and 1 mL of pyridine, and the vial was sealed. After the mixture was stirred at room temperature for 72 h, it was cooled to room temperature. A 5 mL amount of CH_2Cl_2 was added, and the solution was washed with distilled H_2O and evaporated at reduced pressure. The residue was separated by silica gel column chromatography, using *n*-hexane−acetone (5:1 → 1:1), followed by purification by passage over a Sephadex LH-20 column, eluted with CH_2Cl_2−MeOH (1:1), and 5.0 mg (0.0058 mmol) of **2** (32.1%) and 2.0 mg (0.0022 mmol) of **3** (12.1%) were afforded. Using the same procedure, with 26.8 mg (0.034 mmol) of (+)-digoxin (**1**) being reacted with 1 mL of Ac_2O and 200 μL of pyridine at 70 °C for 2 h, 24.6 mg (0.025 mmol) of compound **4** (71.9%) was produced.

*(+)-12,4′c-Di-O-acetyldigoxin (**2**):* amorphous, colorless powder; $[\alpha]^{20}_D$ +33 (*c* 0.04, MeOH); UV (MeOH) λ_{max} (log ε) 210 (4.17) nm; ECD (MeOH, nm) λ_{max} ($\Delta\varepsilon$) 221.4 (+5.53); IR (dried film) ν_{max} 3479, 1738, 1620, 1371, 1242, 1165, 1070, 860 cm^{-1}; ^{1}H and ^{13}C NMR data, see Tables S1 and S2 (Supporting Information); positive-ion HRESIMS *m*/*z* 887.4441, calcd for $C_{45}H_{68}O_{16}Na^+$, 887.4400.

*(+)-12,3′c,4′c-Tri-O-acetyldigoxin (**3**):* amorphous, colorless powder; $[\alpha]^{20}_D$ +40 (*c* 0.03, MeOH); UV (MeOH) λ_{max} (log ε) 211 (4.29) nm; ECD (MeOH, nm) λ_{max} ($\Delta\varepsilon$) 213.5 (+4.88); IR (dried film) ν_{max} 3495, 1747, 1628, 1557, 1372, 1246, 1165, 1076, 856 cm^{-1}; ^{1}H and ^{13}C NMR data, see Tables S1 and S2 (Supporting Information); positive-ion HRESIMS *m*/*z* 929.4492, calcd for $C_{47}H_{70}O_{17}Na^+$, 929.4505.

*(+)-12,3′a,3′b,3′c,4′c-Penta-O-acetyldigoxin (**4**):* amorphous, colorless powder; $[\alpha]^{20}_D$ +54 (*c* 0.1, MeOH); UV (MeOH) λ_{max} (log ε) 215 (4.30) nm; ECD (MeOH, nm) λ_{max} ($\Delta\varepsilon$) 219.0 (+10.26); IR (dried film) ν_{max} 3501, 1747, 1634, 1371, 1246, 1156, 1058, 950 cm^{-1}; ^{1}H and ^{13}C NMR data, see Tables S1 and S2 (Supporting Information); positive-ion HRESIMS *m*/*z* 1013.4761, calcd for $C_{51}H_{74}O_{19}Na^+$, 1013.4717.

Acid Hydrolysis of (+)-Digoxin (1). To a 25 mL glass vial equipped with a magnetic stirrer, containing 126.4 mg (0.16 mmol) of (+)-digoxin (**1**), was added 8 mL of concentrated HCl, and the vial was sealed. After the mixture was stirred at room temperature overnight, 5 mL of CH_2Cl_2 was added. The solution was washed with H_2O, and the organic layer was evaporated at reduced pressure. The residue was separated by silica gel column chromatography using *n*-hexane−acetone (5:1 → 1:1), followed by purification using a Sephadex LH-20 column, eluted with CH_2Cl_2−MeOH (1:1), and 5.0 mg (0.013 mmol) of **5** (7.9%) and 2.0 mg (0.0054 mmol) of **6** (3.3%) were yielded.

*(+)-Digoxigenin (**5**):* amorphous, colorless powder; $[\alpha]^{20}_D$ +22 (*c* 0.1, MeOH); UV (MeOH) λ_{max} (log ε) 216 (3.92) nm; ECD (MeOH, nm) λ_{max} ($\Delta\varepsilon$) 235.5 (+4.54); IR (dried film) ν_{max} 3390, 1732, 1622, 1446, 1382, 1028, 958, 865 cm^{-1}; ^{1}H and ^{13}C NMR data, see Tables S1 and S2 (Supporting Information); positive-ion HRESIMS *m*/*z* 413.2336, calcd for $C_{23}H_{34}O_5Na^+$, 413.2299.

*(+)-8(9)-β-Anhydrodigoxigenin (**6**):* amorphous, colorless powder; $[\alpha]^{20}_D$ +30 (*c* 0.1, MeOH); UV (MeOH) λ_{max} (log ε) 210 (3.97) nm; ECD (MeOH, nm) λ_{max} ($\Delta\varepsilon$) 216.1 (+5.44), 241.8 (−2.58); IR (dried film) ν_{max} 3418, 1739, 1621, 1444, 1368, 1022, 901, 846 cm^{-1}; ^{1}H and ^{13}C NMR data, see Tables S1 and S2 (Supporting Information); positive-ion HRESIMS *m*/*z* 395.2211, calcd for $C_{23}H_{32}O_4Na^+$, 395.2193.

Alkaline Hydrolysis of (+)-Digoxin (1). To a 25 mL glass vial equipped with a magnetic stirrer, containing 10.8 mg (0.014 mmol) of (+)-digoxin (**1**), was added 8 mL of MeOH saturated with NaOH, and the vial was sealed. After the mixture was stirred at 60 °C overnight, the mixture was acidified with 1 N HCl solution to a pH value of 7.0. The mixture was extracted with CH_2Cl_2, and the CH_2Cl_2 partition was washed with H_2O. The CH_2Cl_2 solution was evaporated at reduced pressure, and the residue was separated by silica gel column chromatography using *n*-hexane−acetone (5:1 → 1:1), followed by purification over a Sephadex LH-20 column, eluted with a mixture of CH_2Cl_2 and MeOH (1:1) to afford 7.0 mg (0.0088 mmol) of **7** (63.3%).

*(+)-17-epi-20,22-Dihydro-21α-hydroxydigoxin (**7**):* amorphous, colorless powder; $[\alpha]^{20}_D$ +16 (*c* 0.1, MeOH); IR (dried film) ν_{max} 3445, 1725, 1458, 1375, 1161, 1067, 939, 867 cm^{-1}; ^{1}H and ^{13}C NMR data, see Table 1; positive-ion HRESIMS *m*/*z* 821.4299, calcd for $C_{41}H_{66}O_{15}Na^+$, 821.4294.

Cell Lines. All cell lines were purchased from the American Type Culture Collection (ATCC, Manassas, VA, USA) and cultured at 37 °C in 5% CO_2. The human HT-29 colon, MDA-MB-231 breast, and OVCAR3 ovarian cancer and MDA-MB-435 melanoma cell lines were cultured in RPMI 1640 medium, supplemented with FBS (10%), penicillin (100 units/mL), and streptomycin (100 μg/mL). The H1299 human non-small-cell lung cancer cell line was maintained in Dulbecco's modified Eagle medium (DMEM containing 25 mM glucose) supplemented with FBS (10%), penicillin (100 units/mL), and streptomycin (100 μg/mL).

Cytotoxicity Assays. The cytotoxicity of the cardiac glycosides was screened against the human cancer HT-29, MDA-MB-231, MDA-MB-435, or OVCAR3 cell lines, with a procedure reported previously,[27,28] with the vehicle and paclitaxel used as the negative and positive control, respectively. Briefly, after log-phase-growth, cells were seeded in 96-well clear flat-bottomed plates (Microtest 96, Falcon) and treated with a test sample or paclitaxel (both dissolved in DMSO and diluted to different concentrations required) or the vehicle (DMSO) for 72 h. Viability of cells was evaluated using a commercial absorbance assay (CellTiter 96 AQueous One Solution Cell Proliferation Assay, Promega Corp, Madison, WI, USA), with the IC_{50} values calculated from the vehicle control. For cytotoxicity testing against the H1299 human non-small-cell lung cancer cell line, cell proliferation was assessed using the MTT proliferation assay kit (Cayman Chemical, Ann Arbor, MI, USA). Cells were seeded in each well of a 96-well plate and treated with the samples for 24 h followed by a treatment with MTT for 4 h. The medium was removed, and 100 μL of Crystal Dissolving Solution was added to each well. The absorbance of the solution was measured at 570 nm, with IC_{50} values calculated from the vehicle control.

Molecular Modeling. For the docking profiles shown in Figure 2, the chain A of the crystal structure 4RET [(+)-digoxin] was used as the receptor, which was prepared by MGLTools[55] to add nonpolar hydrogens and charges. The 3D structure of (+)-17-*epi*-20,22-dihydro-21α-hydroxydigoxin (**7**) was built in Maestro and prepared by LigPrep from Schrodinger Suite 2018-2 [Schrödinger Suite 2018-2

https://dx.doi.org/10.1021/acs.jnatprod.9b01060
J. Nat. Prod. XXXX, XXX, XXX−XXX

Protein Preparation Wizard (Schrödinger, LLC, New York, NY, 2018)]. The geometric optimization was performed using the OPLS3 (optimized potentials for liquid simulation 3) force field with all possible ionization states at pH 7.4 ± 0.1 created by Epik [a software program for p*K*(a) prediction and protonation state generation].[56] Sixteen conformations of **7** generated by LigPrep were used for the molecular docking against the receptor by Autodock Vina.[57,58] A rectangular box (25 × 25 × 30 Å^3) centered around the center of Leu793, Ile787, Glu117, and Gln111 defines the region that the ligands can explore, which could cover nearly all of the α-M1−M6 of Na^+/K^+-ATPase. The top ranked 20 binding poses for each ligand conformation, totally 320 poses, were selected for the further analysis. (+)-Digoxin (**1**) was also docked to the receptor as the reference.

For molecular modeling shown in Figure S11 (Supporting Information), proteins and ligands were prepared from Schrödinger Release 2016-1 [Schrödinger Release 2016-1 Protein Preparation Wizard, Epik version 3.5, Impact version 7.0, Prime version 4.3 (Schrödinger, 2016)]. The Protein Preparation Wizard was used to optimize the crystal structure of the Na^+/K^+-ATPase in complex with (+)-digoxin (PDB code 4RET). Restrained minimization was performed on the hydrogens, with the root-mean-square deviation (RMSD) of heavy atoms being converged to less than 0.30 Å, using the OPLS3 force field. The 3D structure of **7a** with defined stereogenic atoms was built in Maestro by modifying the 3D crystal structure of (+)-digoxin (**1**) (Schrödinger Release 2016-1: Ligprep, version 3.7, Schrödinger, 2016). OPLS3 was used for ligand geometric optimization, with all possible ionization states created at pH 7.4 by Epik (Schrödinger Release 2016-1: Epik, version 3.5, Schrödinger, 2016). All the stereogenic atoms were kept during LigPrep, and default values were utilized for other parameters for protein and ligand preparations. Molecular docking was performed using GOLD v5.2.2[59] with the above prepared protein and ligands. The active site for Na^+/K^+-ATPase was defined as being within 10 Å around the catalytic site in the prepared protein. The best scoring pose for each compound was selected for further analysis, and illustrations were made using Chimera.[60]

Na^+/K^+-ATPase Activity Assay. Na^+/K^+-ATPase activity was assessed using a luminescent ADP detection assay (ADP-Glo Max Assay; Promega) that measures enzymatic activity by quantitating the ADP produced during the enzymatic first half-reaction.[28] Specifically, 10 μL of assay buffer containing adenosine 5′-triphosphatase (ATP) from porcine cerebral cortex (Sigma) was added to the wells of a 96-well plate followed by 10 μL of DMSO or the test compounds dissolved in DMSO. After 5.0 μL of ATP was added to each well followed by a 15 min incubation, 25 μL of ADP-Glo Reagent was added. After a 40 min incubation, 50 μL of kinase detection reagent was added to each well followed by a 60 min incubation. ATP was measured via a luciferin/luciferase reaction using a Synergy Mx (BioTek, Winooski, VT, USA) to assess luminescence.

Glucose Uptake Assay. Using a reported protocol,[52,61] after H1299 cells grown in 24-well plates were washed and treated with FBS-free DMEM for 1.5 h, the cells were subsequently washed and incubated for 30 min in glucose-free KRP buffer. WZB117 (used as the positive control) or (+)-digoxin was added to cells at a final concentration of 30 μM. The cells were incubated for 15 min, and glucose uptake was initiated by adding 37 MBq/L 2-deoxy-D-[^{3}H]glucose and 1 mM regular glucose as the final concentrations to cells. After 40 min of incubation, the glucose uptake was terminated by phosphate-buffered saline. Cells were lysed, and the radioactivity retained in the cell lysates was measured by an LS 6000 series liquid scintillation counter (Beckman Coulter, Inc., Fullerton, CA, USA). The data were analyzed statistically using the Student's *t* test, by comparison of the data from the experimental samples with those from the vehicle control, and $p < 0.05$ was set as the level of significant difference.

Statistical Analysis. The in vitro measurements were performed in triplicate and are representative of three independent experiments, where the values generally agreed within 10%. The dose−response curve was calculated for IC_{50} determinations using nonlinear regression analysis (Table Curve2DV4; AISN Software Inc., Mapleton, OR, USA). Differences among samples were assessed by one-way ANOVA followed by Tukey−Kramer's test, and the significance level was set at $p < 0.05$.

■ ASSOCIATED CONTENT

Supporting Information

The Supporting Information is available free of charge at https://pubs.acs.org/doi/10.1021/acs.jnatprod.9b01060.

Mass and NMR spectra of compounds **1**−**7**; diagrams of COSY, key HMBC, and selective NOESY correlations of compounds **1**−**7**; assignments of the ^{1}H and ^{13}C NMR data of the known compounds **2**−**5**; cytotoxicity toward human cancer cells of **1**−**7**, and analytical data of the known compound **1** (PDF)

■ AUTHOR INFORMATION

Corresponding Author

A. Douglas Kinghorn − *Division of Medicinal Chemistry and Pharmacognosy, College of Pharmacy, The Ohio State University, Columbus, Ohio 43210, United States;* orcid.org/0000-0002-6647-8707; Phone: +1 (614) 247-8094; Email: kinghorn.4@osu.edu; Fax: +1 (614) 247-8642

Authors

Yulin Ren − *Division of Medicinal Chemistry and Pharmacognosy, College of Pharmacy, The Ohio State University, Columbus, Ohio 43210, United States*

Hennrique T. Ribas − *Division of Medicinal Chemistry and Pharmacognosy, College of Pharmacy, The Ohio State University, Columbus, Ohio 43210, United States*

Kimberly Heath − *Department of Pharmaceutical Sciences, College of Pharmacy, University of Illinois at Chicago, Chicago, Illinois 60612, United States*

Sijin Wu − *Division of Medicinal Chemistry and Pharmacognosy, College of Pharmacy, The Ohio State University, Columbus, Ohio 43210, United States*

Jinhong Ren − *Center for Biomolecular Sciences, College of Pharmacy, University of Illinois at Chicago, Chicago, Illinois 60612, United States*

Pratik Shriwas − *Department of Biological Sciences, Edison Biotechnology Institute, and Molecular and Cellular Biology Program, Ohio University, Athens, Ohio 45701, United States*

Xiaozhuo Chen − *Department of Biological Sciences, Edison Biotechnology Institute, Molecular and Cellular Biology Program, and Department of Biomedical Sciences, Ohio University, Athens, Ohio 45701, United States*

Michael E. Johnson − *Department of Pharmaceutical Sciences, College of Pharmacy and Center for Biomolecular Sciences, College of Pharmacy, University of Illinois at Chicago, Chicago, Illinois 60612, United States*

Xiaolin Cheng − *Division of Medicinal Chemistry and Pharmacognosy, College of Pharmacy, The Ohio State University, Columbus, Ohio 43210, United States;* orcid.org/0000-0002-7396-3225

Joanna E. Burdette − *Department of Pharmaceutical Sciences, College of Pharmacy, University of Illinois at Chicago, Chicago, Illinois 60612, United States;* orcid.org/0000-0002-7271-6847

Complete contact information is available at: https://pubs.acs.org/10.1021/acs.jnatprod.9b01060

https://dx.doi.org/10.1021/acs.jnatprod.9b01060
J. Nat. Prod. XXXX, XXX, XXX−XXX

Notes

The authors declare no competing financial interest.

■ ACKNOWLEDGMENTS

This investigation was supported by grant P01 CA125066 funded by the National Cancer Institute, NIH, Bethesda, MD. We thank Dr. David J. Hart, Emeritus Professor, Department of Chemistry and Biochemistry, The Ohio State University, for many helpful comments and suggestions about the mechanism of the formation of compound 7. Dr. Chunhua Yuan, Nuclear Magnetic Resonance Laboratory, and Drs. Arpad Somogy and Nanette M. Kleinholz, Mass Spectrometry and Proteomics, Campus Chemical Instrument Center, The Ohio State University, are acknowledged for their assistance with NMR and MS data collection. Drs. Craig A. McElroy and Deepa Krishnan, College of Pharmacy, The Ohio State University, are thanked for providing access to some of the NMR instrumentation used in this investigation.

■ REFERENCES

(1) Diederich, M.; Muller, F.; Cerella, C. *Biochem. Pharmacol.* **2017**, *125*, 1−11.
(2) Botelho, A. F. M.; Pierezan, F.; Soto-Blanco, B.; Melo, M. M. *Toxicon* **2019**, *158*, 63−68.
(3) Smith, S. *J. Chem. Soc.* **1930**, 508−510.
(4) Go, K.; Kartha, G.; Chen, J. P. *Acta Crystallogr., Sect. B: Struct. Crystallogr. Cryst. Chem.* **1980**, *B36*, 1811−1819.
(5) Ambrosy, A. P.; Butler, J.; Ahmed, A.; Vaduganathan, M.; van Veldhuisen, D. J.; Colucci, W. S.; Gheorghiade, M. J. *J. Am. Coll. Cardiol.* **2014**, *63*, 1823−1832.
(6) Platz, E. A.; Yegnasubramanian, S.; Liu, J. O.; Chong, C. R.; Shim, J. S.; Kenfield, S. A.; Stampfer, M. J.; Willett, W. C.; Giovannucci, E.; Nelson, W. G. *Cancer Discovery* **2011**, *1*, 68−77.
(7) Ren, Y.; Carcache de Blanco, E. J.; Fuchs, J. R.; Soejarto, D. D.; Burdette, J. E.; Swanson, S. M.; Kinghorn, A. D. *J. Nat. Prod.* **2019**, *82*, 657−679.
(8) Johansson, S.; Lindholm, P.; Gullbo, J.; Larsson, R.; Bohlin, L.; Claeson, P. *Anti-Cancer Drugs* **2001**, *12*, 475−483.
(9) Pereira, D. G.; Salgado, M. A. R.; Rocha, S. C.; Santos, H. L.; Villar, J. A. F. P.; Contreras, R. G.; Fontes, C. F. L.; Barbosa, L. A.; Cortes, V. F. *J. Cell. Biochem.* **2018**, *119*, 3352−3362.
(10) Pereira, D. G.; Rendeiro, M. M.; Cortes, V. F.; Barbosa, L. A.; Quintas, L. E. M. *J. Cell. Biochem.* **2019**, *120*, 13107−13114.
(11) Alevizopoulos, K.; Calogeropoulou, T.; Lang, F.; Stournaras, C. *Curr. Drug Targets* **2014**, *15*, 988−1000.
(12) Wang, Y.; Qiu, Q.; Shen, J.-J.; Li, D.-D.; Jiang, X.-J.; Si, S.-Y.; Shao, R.-G.; Wang, Z. *Int. J. Biochem. Cell Biol.* **2012**, *44*, 1813−1824.
(13) Menger, L.; Vacchelli, E.; Adjemian, S.; Martins, I.; Ma, Y.; Shen, S.; Yamazaki, T.; Sukkurwala, A. Q.; Michaud, M.; Mignot, G.; Schlemmer, F.; Sulpice, E.; Locher, C.; Gidrol, X.; Ghiringhelli, F.; Modjtahedi, N.; Galluzzi, L.; André, F.; Zitvogel, L.; Kepp, O.; Kroemer, G. *Sci. Transl. Med.* **2012**, *4*, 143ra99.
(14) Gayed, B. A.; O'Malley, K. J.; Pilch, J.; Wang, Z. *Clin. Transl. Sci.* **2012**, *5*, 39−42.
(15) Wang, T.; Xu, P.; Wang, F.; Zhou, D.; Wang, R.; Meng, L.; Wang, X.; Zhou, M.; Chen, B.; Ouyang, J. *Leuk. Lymphoma* **2017**, *58*, 1673−1685.
(16) Huang, L.; Injac, S. G.; Cui, K.; Braun, F.; Lin, Q.; Du, Y.; Zhang, H.; Kogiso, M.; Lindsay, H.; Zhao, S.; Baxter, P.; Adekunle, A.; Man, T.-K.; Zhao, H.; Li, X.-N.; Lau, C. C.; Wong, S. T. C. *Sci. Transl. Med.* **2018**, *10*, No. eaat0150.
(17) Kaapu, K. J.; Rantaniemi, L.; Talala, K.; Taari, K.; Tammela, T. L. J.; Auvinen, A.; Murtola, T. J. *Sci. Rep.* **2018**, *8*, 10308.
(18) Cornelius, F.; Kanai, R.; Toyoshima, C. *J. Biol. Chem.* **2013**, *288*, 6602−6616.
(19) Khatri, H. R.; Bhattarai, B.; Kaplan, W.; Li, Z.; Curtis Long, M. J.; Aye, Y.; Nagorny, P. *J. Am. Chem. Soc.* **2019**, *141*, 4849−4860.
(20) Langenhan, J. M.; Peters, N. R.; Guzei, I. A.; Hoffmann, F. M.; Thorson, J. S. *Proc. Natl. Acad. Sci. U. S. A.* **2005**, *102*, 12305−12310.
(21) Li, X.-S.; Ren, Y.-C.; Bao, Y.-Z.; Liu, J.; Zhang, X.-K.; Zhang, Y.-W.; Sun, X.-L.; Yao, X.-S.; Tang, J.-S. *Eur. J. Med. Chem.* **2018**, *145*, 252−262.
(22) Winnicka, K.; Bielawski, K.; Bielawska, A.; Surażyński, A. *Biol. Pharm. Bull.* **2008**, *31*, 1131−1140.
(23) Huh, J. R.; Leung, M. W. L.; Huang, P.; Ryan, D. A.; Krout, M. R.; Malapaka, R. R. V; Chow, J.; Manel, N.; Ciofani, M.; Kim, S. V.; Cuesta, A.; Santori, F. R.; Lafaille, J. J.; Xu, H. E.; Gin, D. Y.; Rastinejad, F.; Littman, D. R. *Nature* **2011**, *472*, 486−490.
(24) Alves, S. L. G.; Paixão, N.; Ferreira, L. G. R.; Santos, F. R. S.; Neves, L. D. R.; Oliveira, G. C.; Cortes, V. F.; Salomé, K. S.; Barison, A.; Santos, F. V.; Cenzi, G.; Varotti, F. P.; Oliveira, S. M. F.; Taranto, A. G.; Comar, M.; Silva, L. M.; Noël, F.; Quintas, L. E. M.; Barbosa, L. A.; Villar, J. A. F. P. *Bioorg. Med. Chem.* **2015**, *23*, 4397−4404.
(25) Rocha, S. C.; Pessoa, M. T. C.; Neves, L. D. R.; Alves, S. L. G.; Silva, L. M.; Santos, H. L.; Oliveira, S. M. F.; Taranto, A. G.; Comar, M.; Gomes, I. V.; Santos, F. V.; Paixão, N.; Quintas, L. E. M.; Noël, F.; Pereira, A. F.; Tessis, A. C. S. C.; Gomes, N. L. S.; Moreira, O. C.; Rincon-Heredia, R.; Varotti, F. P.; Blanco, G.; Villar, J. A. F. P.; Contreras, R. G.; Barbosa, L. A. *PLoS One* **2014**, *9*, No. e108776.
(26) Kinghorn, A. D.; Carcache de Blanco, E. J.; Lucas, D. M.; Rakotondraibe, H. L.; Orjala, J.; Soejarto, D. D.; Oberlies, N. H.; Pearce, C. J.; Wani, M. C.; Stockwell, B. R.; Burdette, J. E.; Swanson, S. M.; Fuchs, J. R.; Phelps, M. A.; Xu, L.; Zhang, X.; Shen, Y. Y. *Anticancer Res.* **2016**, *36*, 5623−5637.
(27) Ren, Y.; Chen, W.-L.; Lantvit, D. D.; Sass, E. J.; Shriwas, P.; Ninh, T. N.; Chai, H.-B.; Zhang, X.; Soejarto, D. D.; Chen, X.; Lucas, D. M.; Swanson, S. M.; Burdette, J. E.; Kinghorn, A. D. *J. Nat. Prod.* **2017**, *80*, 648−658.
(28) Chen, W.-L.; Ren, Y.; Ren, J.; Erxleben, C.; Johnson, M. E.; Gentile, S.; Kinghorn, A. D.; Swanson, S. M.; Burdette, J. E. *J. Nat. Prod.* **2017**, *80*, 659−669.
(29) Anaya-Eugenio, G. D.; Addo, E. M.; Ezzone, N.; Henkin, J. M.; Ninh, T. N.; Ren, Y.; Soejarto, D. D.; Kinghorn, A. D.; Carcache de Blanco, E. J. *J. Nat. Prod.* **2019**, *82*, 1645−1655.
(30) Maerten, V. G.; Haberland, G. *Arzneim.-Forsch.* **1970**, *20*, 347−351.
(31) Gottlieb, H. E.; Kotlyar, V.; Nudelman, A. *J. Org. Chem.* **1997**, *62*, 7512−7515.
(32) Aulabaugh, A. E.; Crouch, R. C.; Martin, G. E.; Ragouzeos, A.; Shockcor, J. P.; Spitzer, T. D.; Farrant, R. D.; Hudson, B. D.; Lindon, J. C. *Carbohydr. Res.* **1992**, *230*, 201−212.
(33) Cardwell, H. M. E.; Smith, S. *J. Chem. Soc.* **1954**, 2012−2023.
(34) Drakenberg, T.; Brodelius, P.; McIntyre, D. D.; Vogel, H. J. *Can. J. Chem.* **1990**, *68*, 272−277.
(35) Hanna, A. G.; Elgamal, M. H. A.; Morsy, N. A. M.; Duddeck, H.; Kovács, J.; Tóth, G. *Magn. Reson. Chem.* **1999**, *37*, 754−757.
(36) Araya, J. J.; Kindscher, K.; Timmermann, B. N. *J. Nat. Prod.* **2012**, *75*, 400−407.
(37) Ogawa, H.; Shinoda, T.; Cornelius, F.; Toyoshima, C. *Proc. Natl. Acad. Sci. U. S. A.* **2009**, *106*, 13742−13747.
(38) Laursen, M.; Yatime, L.; Nissen, P.; Fedosova, N. U. *Proc. Natl. Acad. Sci. U. S. A.* **2013**, *110*, 10958−10963.
(39) Laursen, M.; Gregersen, J. L.; Yatime, L.; Nissen, P.; Fedosova, N. U. *Proc. Natl. Acad. Sci. U. S. A.* **2015**, *112*, 1755−1760.
(40) Paula, S.; Tabet, M. R.; Ball, W. J. *Biochemistry* **2005**, *44*, 498−510.
(41) Barratt, E.; Bronowska, A.; Vondrášek, J.; Černý, J.; Bingham, R.; Phillips, S.; Homans, S. W. *J. Mol. Biol.* **2006**, *362*, 994−1003.
(42) Noël, F.; Azalim, P.; do Monte, F. M.; Quintas, L. E. M.; Katz, A.; Karlish, S. J. D. *J. Pharmacol. Toxicol. Methods* **2018**, *94*, 64−72.
(43) Stanton, D. T.; Ankenbauer, J.; Rothgeb, D.; Draper, M.; Paula, S. *Bioorg. Med. Chem.* **2007**, *15*, 6062−6070.
(44) Patel, S. *Biomed. Pharmacother.* **2016**, *84*, 1036−1041.
(45) Wright, E. M.; Loo, D. D. F.; Hirayama, B. A. *Physiol. Rev.* **2011**, *91*, 733−794.

https://dx.doi.org/10.1021/acs.jnatprod.9b01060
J. Nat. Prod. XXXX, XXX, XXX−XXX

(46) Thorsen, K.; Drengstig, T.; Ruoff, P. *Am. J. Physiol. Cell Physiol.* **2014**, *307*, C320−C337.
(47) Waller, A. P.; Kalyanasundaram, A.; Hayes, S.; Periasamy, M.; Lacombe, V. A. *Biochim. Biophys. Acta, Mol. Basis Dis.* **2015**, *1852*, 873−881.
(48) Csáky, T. Z.; Hartzog, H. G.; Fernald, G. W. *Am. J. Physiol.* **1961**, *200*, 459−460.
(49) Warburg, O. *Science* **1956**, *123*, 309−314.
(50) Granchi, C.; Fancelli, D.; Minutolo, F. *Bioorg. Med. Chem. Lett.* **2014**, *24*, 4915−4925.
(51) Qian, Y.; Wang, X.; Chen, X. *World J. Transl. Med.* **2014**, *3*, 37−57.
(52) Ren, Y.; Yuan, C.; Qian, Y.; Chai, H.-B.; Chen, X.; Goetz, M.; Kinghorn, A. D. *J. Nat. Prod.* **2014**, *77*, 550−556.
(53) Kupfer, S.; Kosovsky, J. D. *J. Clin. Invest.* **1965**, *44*, 1132−1143.
(54) Eichhorn, E. J.; Gheorghiade, M. *Prog. Cardiovasc. Dis.* **2002**, *44*, 251−266.
(55) Goodsell, D. S.; Morris, G. M.; Olson, A. J. *J. Mol. Recognit.* **1996**, *9*, 1−5.
(56) Shelley, J. C.; Cholleti, A.; Frye, L. L.; Greenwood, J. R.; Timlin, M. R.; Uchimaya, M. *J. Comput.-Aided Mol. Des.* **2007**, *21*, 681−691.
(57) Trott, O.; Olson, A. J. *J. Comput. Chem.* **2009**, *31*, 455−461.
(58) Seeliger, D.; Groot, B. L. *J. Comput.-Aided Mol. Des.* **2010**, *24*, 417−422.
(59) Verdonk, M. L.; Cole, J. C.; Hartshorn, M. J.; Murray, C. W.; Taylor, R. D. *Proteins: Struct., Funct., Genet.* **2003**, *52*, 609−623.
(60) Pettersen, E. F.; Goddard, T. D.; Huang, C. C.; Couch, G. S.; Greenblatt, D. M.; Meng, E. C.; Ferrin, T. E. *J. Comput. Chem.* **2004**, *25*, 1605−1612.
(61) Liu, Y.; Cao, Y.; Zhang, W.; Bergmeier, S.; Qian, Y.; Akbar, H.; Colvin, R.; Ding, J.; Tong, L.; Wu, S.; Hines, J.; Chen, X. *Mol. Cancer Ther.* **2012**, *11*, 1672−1682.

https://dx.doi.org/10.1021/acs.jnatprod.9b01060
J. Nat. Prod. XXXX, XXX, XXX−XXX